

**Erratum: Gravitational waves from nonspinning black hole-neutron star binaries:
Dependence on equations of state
[Phys. Rev. D **82**, 044049 (2010)]**

Koutarou Kyutoku and Masaru Shibata

Keisuke Taniguchi

(Received 4 August 2011; published 26 August 2011)

DOI: [10.1103/PhysRevD.84.049902](https://doi.org/10.1103/PhysRevD.84.049902)

PACS numbers: 04.25.D-, 04.30.-w, 04.40.Dg, 99.10.Cd

In our original paper, we performed numerical simulations for the merger of a nonspinning black hole (BH) and a neutron star (NS), and explored gravitational waves emitted and the final outcome formed after the merger. We recently noticed that we systematically *underestimated* disk masses in this work. The reason is that we evolved hydrodynamic variables and estimated disk masses only in domains of the size $\sim 200^3$ km³, although Einstein's field equation was solved in domains of the size $\sim 800^3$ km³. A small domain size for hydrodynamics is insufficient for the estimation of the disk mass because, if tidal disruption occurs at a distant orbit, especially for the case in which the NS radius is large (~ 15 km), tidal disrupted material extends far away from the central region. For this reason, we performed again the same simulations as in our original paper, enlarging the computational domain of hydrodynamics. To estimate disk mass more accurately, in addition, we enlarged the size of the computational domain to the size 1500^3 – 2000^3 km³. This is done by increasing a

TABLE I. Setup of the grid structure for the computation with our AMR algorithm. $\Delta x = h_7 = L/(2^7 N)$ is the grid spacing at the finest-resolution domain with L being the location of the outer boundaries for each axis. $R_{\text{diam}}/\Delta x$ denotes the grid number assigned inside the semimajor diameter of the NS. λ_0 is the gravitational wavelength of the initial configuration.

Model	$\Delta x/M_0$	$R_{\text{diam}}/\Delta x$	L/λ_0
2H-Q2M135	0.0471	90.8	2.377
H-Q2M135	0.0377	86.2	2.130
HB-Q2M135	0.0347	87.0	1.963
HBs-Q2M135	0.0353	85.2	1.996
HBss-Q2M135	0.0353	84.0	1.996
B-Q2M135	0.0330	85.1	1.863
Bs-Q2M135	0.0324	84.4	1.830
Bss-Q2M135	0.0270	95.4	1.650
2H-Q3M135	0.0353	89.0	1.996
H-Q3M135	0.0282	84.7	1.711
HB-Q3M135	0.0269	82.7	1.631
B-Q3M135	0.0247	83.8	1.497
2H-Q2M12	0.0565	86.9	2.510
H-Q2M12	0.0453	83.1	2.563
HB-Q2M12	0.0420	83.6	2.377
B-Q2M12	0.0392	83.4	2.218
HB-Q3M12	0.0306	84.6	1.713
B-Q3M12	0.0278	86.9	1.572

coarse domain by one more level in the adaptive mesh refinement algorithm (AMR). Specifically, the number of coarser domains is increased from three to four. Table I (new version of Table III in our original paper) summarizes the parameters of the new grid structure. In these simulations, the total rest mass of the atmosphere is always less than $10^{-4}M_{\odot}$. Results for gravitational waves do not change within the level of numerical accuracy in our simulations.

Table II (corrected version of Table V in our original paper) lists corrected values for quantities associated with the merger remnants. We estimated all the values at the end of the simulations in this paper. In this Erratum, we present the values evaluated at ≈ 10 ms after the merger to perform more systematic comparisons. Quantities associated with the remnant BH do not change appreciably. Taking into account the change in the time at which the disk mass is estimated, the mass of the remnant disk becomes larger by a factor of $\sim 2\text{--}3$ for $Q = 2$ and by a factor of ~ 5 for $Q = 3$. Figure 1 (corrected version of Fig. 12 of our original article) plots the time evolution of $M_{r>r_{\text{AH}}}$. Although qualitative behavior is not altered, $M_{r>r_{\text{AH}}}$ is systematically larger for the new computations. In particular, the sudden decrease of $M_{r>r_{\text{AH}}}$ at $\sim 3\text{--}5$ ms after the merger seen in Fig. 12 of the published article now disappears. Approximate accretion time scale t_{d} becomes longer by a factor of $\lesssim 2$ for many cases. Figure 2 (corrected version of Fig. 13 of the published article) plots the values of $M_{r>r_{\text{AH}}}$ at ≈ 10 ms after the merger as a function of \mathcal{C} . Although we again see the systematic increase of $M_{r>r_{\text{AH}}}$, the conclusion that the disk mass is much smaller than $0.01M_{\odot}$ for BH-NS binaries with the typical NS mass of $M_{\text{NS}} = 1.2\text{--}1.35M_{\odot}$ and $\mathcal{C} \gtrsim 0.16$ does not change [1]. Figure 3 (corrected version of Fig. 14 in the original article) plots the relation between $M_{r>r_{\text{AH}}}$ and the maximum rest mass density ρ_{max} of the remnant disk. Approximately speaking, the relations between them are not changed qualitatively and quantitatively.

Table III (corrected version of Table VI of our original article) lists several numerical results for the merger remnants, and Fig. 4 (corrected version of Fig. 17 in the original article) plots the time evolution of $M_{r>r_{\text{AH}}}$ for different grid resolutions. The convergence of the remnant disk mass becomes slightly better than that in the original article.

TABLE II. Several key quantities for the merger remnants. All the quantities are estimated at $t - t_{\text{merger}} \approx 10$ ms, where t_{merger} denotes the time of the merger. $M_{r>r_{\text{AH}}}$ is the rest mass of the disk surrounding the BH; because the accretion is still ongoing at the end of simulations due to the hydrodynamic angular momentum transport process, the values listed give only an approximate mass of the long-lived accretion disk, which survives for a time scale longer than the dynamical time scale ~ 10 ms. t_{d} is the approximate accretion time scale estimated around ≈ 10 ms after the merger, which we show only for the case $M_{r>r_{\text{AH}}} \gtrsim 0.001M_{\odot}$. C_e and C_p are the circumferential radii of the apparent horizon along the equatorial plane and meridional plane, respectively, and $C_e/4\pi$ is the approximate mass of the remnant BH. M_{irr} is the irreducible mass of the remnant BH. a is the nondimensional spin parameter of the remnant BH estimated from C_p/C_e .

Model	$M_{r>r_{\text{AH}}}[M_{\odot}]$	t_{d} (ms)	$C_e/4\pi M_0$	M_{irr}/M_0	C_p/C_e	a
2H-Q2M135	0.20	57	0.942	0.886	0.913	0.64
H-Q2M135	0.076	32	0.969	0.905	0.903	0.67
HB-Q2M135	0.032	24	0.978	0.912	0.902	0.67
HBs-Q2M135	0.024	22	0.980	0.914	0.902	0.67
HBss-Q2M135	0.014	21	0.980	0.915	0.902	0.67
B-Q2M135	0.0085	18	0.980	0.916	0.904	0.67
Bs-Q2M135	0.0053	23	0.980	0.917	0.906	0.66
Bss-Q2M135	7×10^{-4}	...	0.977	0.917	0.910	0.65
2H-Q3M135	0.19	26	0.958	0.923	0.945	0.52
H-Q3M135	0.013	26	0.982	0.940	0.936	0.56
HB-Q3M135	0.0022	25	0.983	0.941	0.936	0.56
B-Q3M135	2×10^{-4}	...	0.982	0.941	0.938	0.55
2H-Q2M12	0.21	66	0.937	0.885	0.918	0.62
H-Q2M12	0.12	28	0.958	0.900	0.907	0.66
HB-Q2M12	0.091	31	0.965	0.902	0.905	0.66
B-Q2M12	0.065	27	0.970	0.906	0.903	0.67
HB-Q3M12	0.044	30	0.977	0.936	0.937	0.55
B-Q3M12	0.011	28	0.982	0.939	0.935	0.56

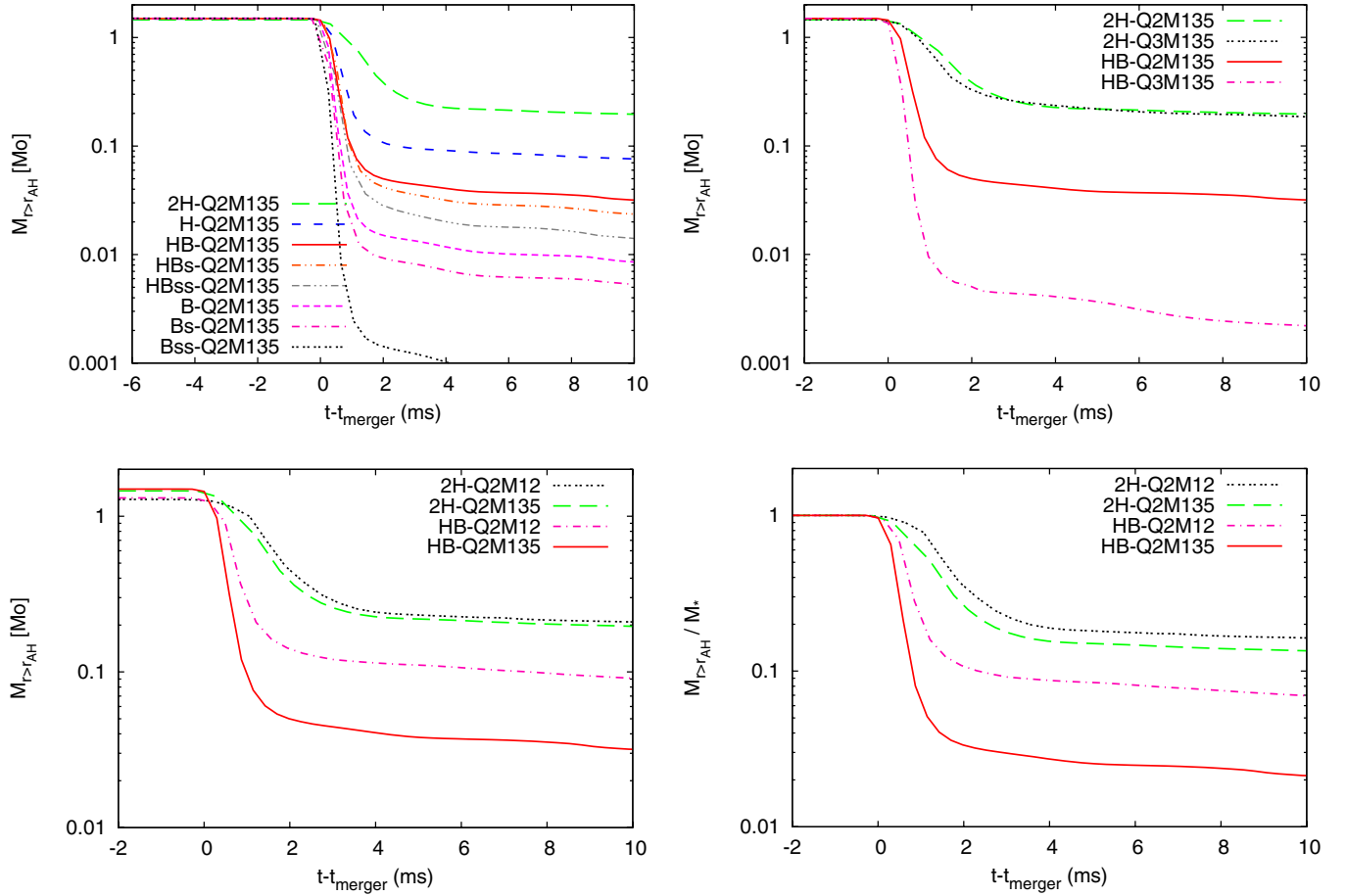


FIG. 1 (color online). Evolution of the rest mass of the material located outside the apparent horizon, $M_{r>r_{\text{AH}}}$, with an appropriate time shift; in these plots, the time at the onset of the merger is taken as the time origin. The top-left panel shows the results for models with $Q = 2$ and $M_{\text{NS}} = 1.35M_{\odot}$ for all the EOSs employed in this paper. The top-right panel shows the results for selected models with $M_{\text{NS}} = 1.35M_{\odot}$ but with different values of Q . The bottom-left panel shows the results for selected models with $Q = 2$ but with the different NS mass M_{NS} . The bottom-right panel is the same as the bottom-left panel except for the normalization of the mass, with respect to the initial rest mass M_* .

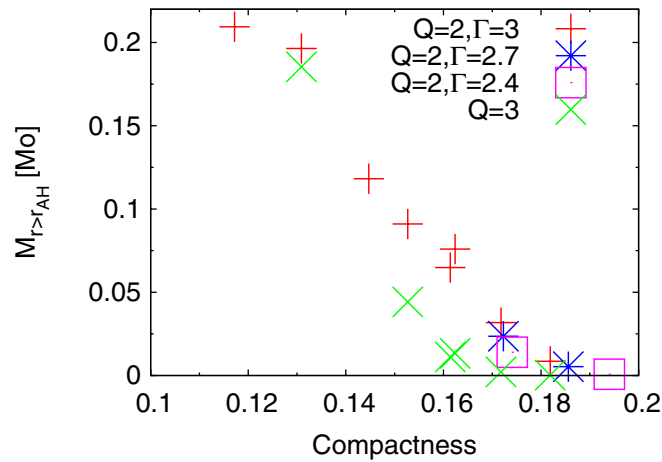


FIG. 2 (color online). Disk mass $M_{r>r_{\text{AH}}}$ at $t - t_{\text{merger}} \approx 10$ ms as a function of the NS compactness \mathcal{C} .

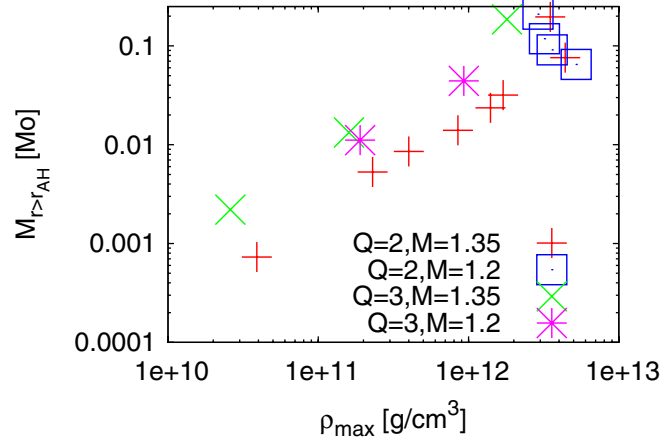


FIG. 3 (color online). Relation between disk mass $M_{r>r_{\text{AH}}}$ and the maximum density, ρ_{max} , estimated at $t - t_{\text{merger}} \approx 10$ ms. The maximum density oscillates with time even in the quasistationary phase, and we here plot a value averaged in one oscillation period.

TABLE III. The disk masses at $t - t_{\text{merger}} \approx 10$ ms and nondimensional spin parameters of the remnant BHs for models HB-Q2M135 and H-Q3M135 with different grid resolutions, $N = 50, 42$, and 36 .

N	$M_{r>r_{\text{AH}}}[M_{\odot}](10 \text{ ms})$	a
HB-Q2M135		
50	0.032	0.67
42	0.031	0.67
36	0.030	0.67
H-Q3M135		
50	0.013	0.56
42	0.013	0.56
36	0.013	0.56

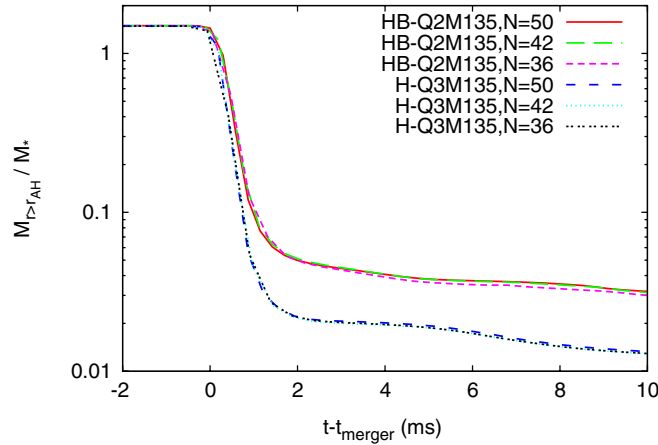


FIG. 4 (color online). Comparison of the disk-mass evolution for models HB-Q2M135 and H-Q3M135 with different grid resolutions.

[1] The sign of $\mathcal{C} \leq 0.16$ and $\mathcal{C} \geq 0.16$ in page 19 of our original paper was opposite.